PRAMANA
— journal of
physics

© Indian Academy of Sciences

Vol. 57, No. 4
October 2001
pp. 763–774

Magnetization curves for general cylindrical samples in a transverse field

K V BHAGWAT and DEBJANI KARMAKAR
Technical Physics and Prototype Engineering Division, Bhabha Atomic Research Centre, Trombay, Mumbai 400 085, India

MS received 1 December 2000; revised 3 March 2001

Abstract. Using the recent results for the surface current density on cylindrical surfaces of arbitrary cross-section producing uniform interior magnetic field we propose a method for obtaining solutions of Bean's critical state model for general cylindrical samples. The method uses the technique of conformal mapping to express the sample surface and the flux-fronts in terms of a set of coefficients that depend on a parameter. The flux-fronts are to be determined by solving a system of nonlinear ordinary differential equations for the coefficients. Retaining only a certain finite number of leading coefficients we get an approximate solution. The procedure is illustrated by considering two cylindrical samples – one with an elliptical cross-section and the other with a non-elliptical cross-section. The virgin curve and small and large magnetization hysteresis loops for the two samples are obtained.

Keywords. Magnetization curves; Bean; critical state model; hysteresis curves.

PACS Nos 74.25.Ha

1. Introduction

Bean [1] proposed the critical state model (CSM) to describe irreversible magnetization of hard type-II superconductors using just one parameter J_c – the critical current density – characterizing the superconductor. Its various extensions and generalizations have been studied in literature including the field-dependent and more recently the history dependent J_c [2]. Starting with the early work of Kato [3] and Wilson [4] efforts have been continuously devoted to study samples with nonzero demagnetization factor ($N \neq 0$). The discovery of high-T_c superconductors has only boosted these studies during the past decade (see ref. [5] for some earlier references). With easy availability of samples in the form of discs and platelets recent experimental and theoretical studies have mainly focussed on thin samples – discs [6] and strips [7] – in the transverse geometry, with applied field perpendicular to thicker dimension. The case of field-dependent J_c in thin samples has been considered by Mc Donald and Clem [8], Bhagwat and Chaddah [9] and more recently by Shantsev *et al* [10]. Theoretical study of thin samples affords one simplification. Here one needs to work only with an 'average' current density, or a current-sheet. The immense complexity associated with the task of determining and studying the movement of the flux-front as the flux penetrates the sample is absent. Bhagwat and Chaddah have also worked

with finite samples and have solved a re-statement of CSM for elliptical cylinders in transverse geometry, for a spheroid [5] and also for the general ellipsoid [11]. Navarro and Campbell [12] have followed a numerical procedure for obtaining flux-fronts and magnetization for a sphere, and oblate and prolate spheroids. Prigozhin [13] has worked out a variational formulation and obtained numerical solution for flux-fronts. To determine the hysteresis loss in superconducting wires, Ashkin [15] has worked out the flux-fronts numerically. Telchow and Koo [16] have provided a numerical solution for the flux-fronts and the magnetization curves for a sphere by solving an integral equation. They observe that for samples with cylindrical symmetry a flux-front can be viewed as a surface of zero vector potential.

More recently, Brandt [14] has extended his earlier solution for thin strips and discs to those having a finite thickness and has worked with a realistic current-voltage law. His solution also involves solving an infinite system of nonlinear differential equations and follows a numerical procedure. However, in his treatment even the various matrix elements need numerical evaluation.

Thus, for samples with $N \neq 0$ there is no direct analytical formulation of the general problem and a method of solution that yields the evolution of flux-fronts as the external field is applied on a zero field cooled virgin sample of a hard type-II superconductor.

In this paper we present such a formulation and a method for solving the CSM for general cylinders, which can, hopefully, be adopted by an interested research worker. Here we have generalized our earlier elementary application of this method [17] based on the assumption of parallel flux-fronts. We employ the recent exact results [18] for surface current density on cylinders of arbitrary cross-section producing uniform interior field. The procedure involves determining the conformal mapping of the exterior of a unit circle on to the exterior of the boundary of the cross-section of the cylinder. The general form of such a mapping is discussed by Polya and Szegö [19]. Starting with the sample surface, the flux-fronts form a one-parameter family of surfaces. A natural choice for the paramater characterizing the family would be the magnitude of the applied field. In general, any function of it should serve the purpose. Since there is some advantage in choosing the latter, we keep this option open. Thus, let ξ denote the parameter describing the family of flux-fronts. The current carrying region of the sample can be divided into a closely spaced succession of flux-fronts. The thin shell of current between consecutive flux fronts can be considered as a surface current on the inner flux-front (of appropriate density). Alternatively, movement of the flux-front can be considered as preceded by setting up an appropriate surface current density (that produces interior field exactly cancelling the change in the external field) on the innermost flux-front which subsequently relaxes into a volume current density causing the flux-front to move by an appropriate amount. Since the flux-front does not retain the shape of the sample we need to know the surface current density on cylinders of arbitrary cross-section.

The paper is organized as follows. In §2 we formulate the problem for determining the flux-front as outlined above such that the volume current density is built out of current shells (or a surface current density). The condition that the current density should be of constant magnitude, equal to J_c leads to an infinite system of nonlinear first order differential equations for the coefficients that appear in the conformal mapping introduced in §2.2. Subsequently we indicate an essential feature of the exact flux-fronts and indicate an approximation procedure by restricting to a number of leading coefficients. In §3 we present expressions for virgin and hysteresis magnetization and the relation between the

applied field and the flux-front parameter ξ_0. In §4 we present the results for two sample shapes and close with a discussion.

2. Formulation

2.1 *Volume current density viewed as a succession of current shells*

Let us consider an infinite cylindrical sample with its axis along the z-axis and its cross-section bounded by a contour **L**. Let the zero field cooled sample be subjected to an uniform magnetic field. The sample responds by setting up a surface current density (parallel to the axis of the cylinder) that generates field that exactly cancels the applied field everywhere within the sample. The surface current density relaxes into a (volume) current density J_c to go into the critical state. Let us now trace back the surface current density from a volume current density $\mathbf{J}(x',y')$. If $\hat{\mathbf{i}}$, $\hat{\mathbf{j}}$ and $\hat{\mathbf{k}}$ denote unit vectors along the co-ordinate axes then the field $\mathbf{B_J}$ generated by $\mathbf{J}$ is given by [20]

$$\mathbf{B_J} = \frac{\mu_0}{2\pi}\int\int \frac{J(x',y')[-(y-y')\hat{\mathbf{i}}+(x-x')\hat{\mathbf{j}}]}{(x-x')^2+(y-y')^2}\mathrm{d}x'\,\mathrm{d}y'. \tag{1}$$

The integration extends over the current carrying region. Introducing a complex function $B_J(\zeta)$, with $\zeta = x+\imath y$, $\zeta' = x'+\imath y'$, [20] we may write

$$B_J(\zeta) = \frac{\mu_0}{2\pi}\int\int \frac{J(x',y')}{\zeta-\zeta'}\mathrm{d}x'\,\mathrm{d}y'. \tag{2}$$

The components of $\mathbf{B_J}$ are obtained as $\mathbf{B_{J}}_x = \mathrm{Im}B_J(\zeta)$ and $\mathbf{B_{J}}_y = \mathrm{Re}B_J(\zeta)$. Effecting a change of variables from ζ' to $(\xi',\ u'=\exp(\imath\phi'))$ by writing $\zeta' = f(\xi',u')$, where f is an analytic function of u', treated as a complex variable. The integral in eq. (2) can be expressed in the form

$$B(\zeta) = \frac{\mu_0}{2\pi}\int \mathrm{d}\xi' \int \frac{J(x',y')}{(\zeta-\zeta')}\,\frac{\chi(\xi',\phi')}{|f'(\xi',u')|}\,\mathrm{d}s'. \tag{3}$$

Here $\chi(\xi',\phi') \equiv x'_{\xi'}y'_{\phi'} - x'_{\phi'}y'_{\xi'}$ is the Jacobian of transformation and $\mathrm{d}s' = |\mathrm{d}\zeta'| = |f'(\xi',u')|\mathrm{d}\phi'$. The net $B(\zeta)$ can be viewed as produced by a succession of current shells of thickness $\mathrm{d}\xi'$. Each current shell carries a surface current density $J_s = J\chi/|f'(\xi',u')|\mathrm{d}\xi'$.

2.2 *Description of flux-fronts by their conformal maps*

Now consider the conformal map [19]

$$\zeta = f(u) = a_0u + a_1u^{-1} + a_2u^{-3} + \cdots. \tag{4}$$

We assume that the coefficients $a_0, a_1, a_2, \ldots$ are real and are such that the zeroes of $f'(u)$ all lie within the unit circle $u = \exp(\imath\phi)$, in the u-plane. Thus the mapping is conformal

for $|u| > 1$, i.e., it maps the exterior of the unit circle to the exterior of a certain curve in the z-plane. Let this curve be the boundary **L** of the cross-section of the cylindrical sample under consideration. As u goes round a unit circle $\zeta = x + \imath y$ describes curve bounding the cylinder cross-section. We assume that various flux-fronts are also described by conformal maps similar to eq. (4). Since the bounding curve and flux-fronts belong to a family of curves characterized by the parameter ξ we can conceive of a family of conformal maps of the type (4). For this family the coefficients (the $\{a$'s$\}$) will be functions of ξ. These would evolve starting from their initial values. It should be noted that without loss of generality we may restrict ξ to the range $(0,1)$ in such a way that $\xi = 1$ corresponds to the boundary **L** of the cylindrical sample. If an external field B_A is applied along x-direction, the current carrying region is bounded by sample surface $\xi = 1$ and a flux-front corresponding to $\xi = \xi_0$, say, which must be related to the applied field B_A.

Let the current carrying region be divided into shells of thickness $\mathrm{d}\xi$, and let the shell $(\xi, \xi + \mathrm{d}\xi)$ carry a 'surface current density' [18]:

$$\mu_0 J_s = 2\delta B_0 a_0 \sin\phi / |f'(u)|, \quad \text{with } u = \exp(\imath\phi). \tag{5}$$

By the results of [18] this shell shall produce a uniform interior field δB_0. A comparison of eqs (5) and (3) implies that the volume current density

$$J\mathrm{d}\xi = \delta B_0 a_0 \sin\phi / \chi \quad \text{with } u = \exp(\imath\phi) \tag{6}$$

shall also produce uniform interior field. For symmetric samples we shall assume that $|J| = J_c$, the critical current density for $\phi = \pi/2$. This enables us to eliminate infinitesimals appearing in eq. (6) and we get

$$J(\xi,\phi) = J_c\, \chi(\xi, \pi/2) \sin\phi / \chi(\xi,\phi). \tag{7}$$

Thus for every pre-assigned (arbitrary) ξ-dependence of the coefficients we can deduce the (volume) current density and also the extent of the current carrying region (limited by the parameter value ξ_0) that will produce uniform interior field B_J exactly cancelling the externally applied uniform field B_A at all points interior to the flux-front. In particular, we can choose the ξ-dependence of the coefficients to make also $|J| = J_c$ everywhere in the current carrying region (except possibly at the poles, i.e., $\phi = 0,\ \pi$).

2.3 *Differential equations for the coefficients*

We have introduced an unspecified parameter ξ, $(0 \le \xi \le 1)$ that labels the family flux-fronts and ξ_0 that labels innermost flux-front is related to the applied field B_A. Based on physical intuition, we now make a specific choice for this parameter by requiring that $b\xi$ represents the transverse (to B_A) dimension of the flux-front, where b is the transverse dimension of the sample. Thus under the mapping (4) we have

$$b\xi = a_0(\xi) - a_1(\xi) + a_2(\xi) - a_3(\xi) + \cdots. \tag{8}$$

From eq. (7) it is clear that the condition $|J| = J_c$ is equivalent to

$$\chi(\xi,\phi) = \chi(\xi,\pi/2)\sin\phi,\ (0 < \phi < \pi). \tag{9}$$

Recalling that χ is the Jacobian involving partial derivatives of x and y (c.f. the text following eq. (3)), the above equation can be readily recognized to be the partial differential equation determining the flux-fronts, the initial condition being that these reduce to the given sample surface. We have a single equation determining two unknown functions which should form the real and imaginary parts of an analytic function. We are unable to find treatment of such equations in books dealing with partial differential equations. We start with the representation (4) itself with the coefficients depending on the variable ξ. Thus x and y have been chosen to be the real and imaginary parts of an analytic function. A straightforward calculation leads to the expression for χ,

$$\chi(\xi,\phi) = -\sum_{m,n=0}^{\infty} (2m-1)a_m a'_n \cos 2(m-n)\phi. \tag{10}$$

Here a'_n denotes derivative of a_n with respect to ξ. We shall use the notation $\chi_0(\xi) = \chi(\xi,\pi/2)$. From eqs (9) and (10) we have

$$\sum_{m=0}^{\infty} (2m-1)a_m a'_n \cos 2(m-n)\phi = -\chi_0 \sin\phi. \tag{11}$$

Setting $\phi = \pi/2$ we get after some rearrangements, an expression for χ_0 solely in terms of the a_n's:

$$\chi(\xi_0) = -b\sum_{m=0}^{\infty} (2m-1)a_m. \tag{12}$$

Multiplying both sides of equation (11) by $\cos 2k\phi$ and integrating over $(0,\pi)$ we get the following infinite system of first order nonlinear differential equations for the coefficients

$$\sum_{m=k}^{\infty} a_{m-k}a'_m(2m-2k-1) + \sum_{m=0}^{\infty} a_{m+k}a'_m(2m+2k-1) = (4/\pi)[\chi_0(\xi)/(4k^2-1)]. \tag{13}$$

To solve these equations we must know the initial values $\{a_n(1), n = 0,1,2,\ldots\}$. These are obtained from eq. (4) by determining the function that maps the exterior of unit circle onto the exterior of the sample boundary **L**. Exact analytical solution of eq. (13) would be difficult and will not be attempted here. An approximate solution can be obtained by suitably truncating the infinite system and determining only a certain number n of leading coefficients. We illustrate the procedure by assuming that $a'_n = 0$, for $n > 20$. The details are worked out for two cylindrical samples.

2.4 *Determination of the flux-front*

The infinite system of differential equations is approximated by a finite system by assuming that only a finite number n of leading coefficients evolve with ξ. We have chosen $n = 20$. We now define the vector $\mathbf{a}^t = (a_0, a_1, \ldots, a_{20})$, and similarly the vector $\mathbf{c}$, with $c_k = 4\chi_0/\pi(4k^2-1)$, for $k = 0, 1, 2, \ldots, 20$ and the matrix $\mathbf{A}$ with elements

$$A_{km} = (2m+2k-1)a_{m+k} + (2m-2k-1)a_{m-k}\Theta(m-k).$$

Here the symbol $\Theta(m-k) = 1$ for $m \geq k$ and zero for $m < k$. The resulting finite system of equations can be cast in the form

$$\mathbf{a}' = \mathbf{A}^{-1}\mathbf{c}.$$

The above equation determines the derivatives $\{a_n'(\xi)\}$ in terms of $a_n(\xi)$. Using the initial values $\{a_n(1)\}$ we have calculated $a_n(\xi)$ at intervals of 0.001. These are used to numerically obtain the virgin and hysteresis magnetization curves. Expressions for virgin and hysteresis magnetization are given below.

3. Virgin and hysteresis magnetization

The relation between the flux-front parameter ξ_0 and the applied field B_A is obtained by writing $B_A = -B_J(\xi_0, 1)$, during the virgin curve. Here $B_J(\xi_0, 1)$ denotes the field within the flux-front generated by the (finite) shell (ξ_0,1) of shielding currents. Thus it is to be noted that even though we have obtained the leading coefficient under the approximation mentioned above $B \equiv 0$ (and not approximately) *everywhere* within the flux-front during the virgin curve. Magnetization is obtained using the relation

$$\mathbf{m}_v = (1/2A)\int\int(\mathbf{r}' \times \mathbf{J})\mathrm{d}x'\,\mathrm{d}y', \tag{14}$$

where A is the cross-sectional area of the sample. Changing the variables of integration to (ξ', ϕ') and noting that the current density is along $\hat{\mathbf{k}}$ we get

$$\mathbf{m}_v = (J_c b/2A)\int_{\xi_0}^{1}\int_{-\pi}^{\pi}\chi_0(\xi')\sin\phi'(\hat{\mathbf{i}}y' - \hat{\mathbf{j}}x')\mathrm{d}\xi'\,\mathrm{d}\phi'. \tag{15}$$

It is clear that only the x-component of the magnetization is non-zero. The cross-sectional area A can be similarly determined,

$$A = \int_0^1\int_{-\pi}^{\pi}\chi(\xi', \phi')\mathrm{d}\xi'\,\mathrm{d}\phi'. \tag{16}$$

The integral can be evaluated in a closed form and we have

$$A = -\pi\sum_{m=0}^{\infty}(2m-1)a_m^2(1).$$

We now give expression for the virgin magnetization and that under field reversal.

3.1 *The virgin curve*

For the virgin curve we have

$$\mu_0 m_v = -(H^*/2A)\int_{\xi_0}^{1}\chi_0(\xi)(a_0 - a_1)\,\mathrm{d}\xi, \tag{17}$$

where $H^* = \mu_0 J_c b$, and

$$B_A = -(H^*/2)\int_{\xi_0}^{1} \chi_0(\xi)/a_0 \, \mathrm{d}\xi. \tag{18}$$

Full field penetration occurs at $\xi = 0$. Beyond full penetration m_v saturates, and B_A is given by

$$B_A = -(H^*/2)\int_{0}^{1} \chi_0(\xi)/a_0 \, \mathrm{d}\xi + B(0), \tag{19}$$

where $B(0)$ is the field at the centre of the sample. The virgin curve merges with the field increasing envelope curve obtained under infinitely large reversal field.

3.2 *Magnetization under field reversal*

For obtaining small hysteresis loops we have the field reversal occurring before full penetration. The decrease in the field changes causes reversal of the direction of the current density in a shell (ξ_0', 1), leaving the current density in the region $\xi_0 < \xi < \xi_0'$ unchanged. The reverse magnetization can be calculated using

$$\mu_0 m\downarrow = \left(\frac{H^*}{2A}\right)\left(-\int_{\xi_0}^{\xi_0'} m(\xi')\,\mathrm{d}\xi' + \int_{\xi_0'}^{1} m(\xi')\,\mathrm{d}\xi'\right), \tag{20}$$

where we have used the symbol $m(\xi') = \chi_0(\xi')(a_0 - a_1)$. The applied field is related to ξ_0 and ξ_0' by the equation

$$B_A = (H^*/2)\left(-\int_{\xi_0}^{\xi_0'} B(\xi')\,\mathrm{d}\xi' + \int_{\xi_0'}^{1} B(\xi')\mathrm{d}\xi'\right), \tag{21}$$

where we have used the definition $B(\xi) = \chi_0((\xi)/a_0)$. For obtaining the large hysteresis loops the reversal field is beyond the field for full penetration. In this case if $B(0)$ is field at the centre of the sample then we have

$$B_A = B(0) + (H^*/2)\left(-\int_{\xi_0}^{\xi_0'} B(\xi')\,\mathrm{d}\xi' + \int_{\xi_0'}^{1} B(\xi')\mathrm{d}\xi'\right). \tag{22}$$

The magnetization is given by

$$\mu_0 m\downarrow = \left(\frac{H^*}{2A}\right)\left(-\int_{0}^{\xi_0'} m(\xi')\,\mathrm{d}\xi' + \int_{\xi_0'}^{1} m(\xi')\,\mathrm{d}\xi'\right). \tag{23}$$

The complete loop is obtained using the symmetry property $m\uparrow(B_A) = -m\downarrow(-B_A)$ of the hysteresis loop. We now present results for two special cylinders.

4. Results and discussion

The exact system of differential equations involves an infinite number of coefficients and it is for this full system that $|J| = J_c$ is obtained. In figure 1 we show how $|J|$ apprroaches J_c as the number of leading coefficients is varied. (It should be noted here that we do not need an explicit solution of the infinite system to get these curves.) It is clear that the value of n should be chosen as large as possible. Obviously computer memory puts a restriction on the magnitude of n. However, even a moderately large n value may result in numerical inaccuracies leading to a set of a_k's that violates the conformal nature of the transformation (cf. eq. (4)). We have chosen $n = 20$, which retains the essential conformal mapping property as well as produces a reasonably good approximation to the current density.

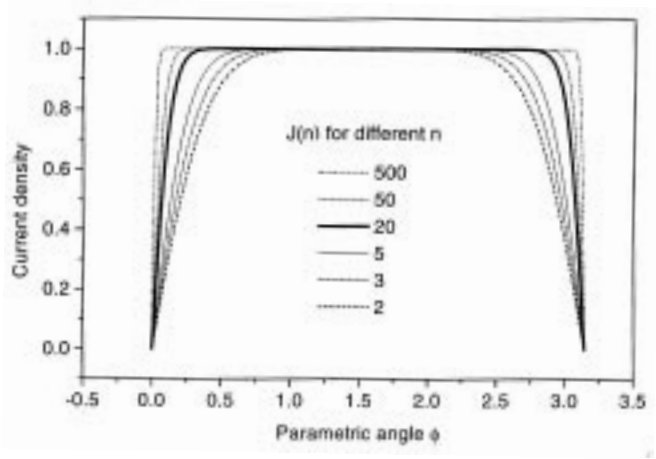

Figure 1. A comparison of current densities for different values of n, the number of leading coefficients used in the conformal mapping. $|J| \to J_c$ as n increases.

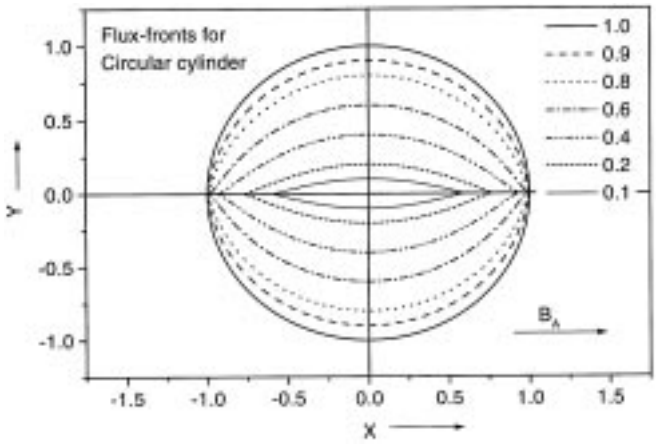

Figure 2. The cross-section and the flux-fronts for a unit circular cylinder are shown for different values of ξ_0.

The case of a circular cylinder is the simplest because in this case the initial conformal mapping is the identity mapping, viz., $\zeta = u$. Under the application of the external field the flux fronts evolve into noncircular shapes. With $n = 20$ we solve the finite system of equations (13) with the initial conditions $a_0(1) = 1$, and $a_n = 0, n \geq 2$. These are shown in figure 2. Here in agreement the results of [12] the flux-fronts initially remain pegged at the poles and develop a 'cusp' which is retained even after its detachment from the poles.

Next we consider an elliptical cylinder with transverse dimension $b = 1$ and the parallel dimension $a = 0.4$. This corresponds to the initial values $a_0(1) = 0.7$ and $a_1(1) = -0.3$ and $a_n(1) = 0$, for $n \geq 2$. We show the flux-fronts in figure 3a. The magnetization curves are shown in figures 3b and 3c.

The cross-section and flux-fronts for the second cylinder are shown in figure 4a. The sample surface corresponds to the initial parameters $a_0(1) = 0.7,\ a_1(1) = -0.35$ and $a_2(1) = -0.05$. These are chosen so that the cylinder has transverse dimension $b = 1$ and parallel dimension $a = 0.3$. The cross-sectional area of the sample $A = 1.131$. The magnetization curves are shown in figures 4b and 4c.

We have also examined the effect of varying n on the shape of the flux-fronts. It was found that the inner flux-fronts corresponding to larger penetration developed a loop in addition to a central simply connected region. At first sight, it appeared that the loops, which are unphysical, must be a result of numerical inaccuracies mentioned above. However, it may be recalled that various flux-fronts are obtained starting from the sample boundary by introducing current shells obtained by redistributing the surface current into a volume current of a constant density J_c. To start with the flux-fronts remain anchored at the 'poles' of the sample. This is because surface current as well as the surface element at the poles both vanish. The surface elements *near* the poles carry small current and give rise to a current shell of small thickness. This shell does not cross the x-axis – the direction of the applied field. As the applied field is increased the shape of the flux-free region becomes more and more spindle-shaped [21]. At a certain stage a small loop is formed near the poles. The loop is formed due to overlapping of current shells that crossed from either side of the x-axis and therefore, must carry zero current. At this stage we may view the zero current density (in the loop region) as coming from current densities $\pm J_c$ in two adjoining regions separated along the x-axis. This redistribution of current density at the infinitesimal level does not alter the fields at finite distances, however adds to sample magnetization a contribution of the same order as coming from the shell. Thus for a given applied field, the resulting sample magnetization is more for this latter situation and this state should prevail in a realistic field penetration. Thus, the redistribution of current density near poles results in the detachment of flux-front from the poles at higher fields. This result is also arrived at in ref. [21] following a different approach.

As noted earlier, we can generate a series of approximate solutions depending on how we truncate the system of equations (13). All these solutions correspond to having $B \equiv 0$ within the innermost flux-front, however, $|J| \neq J_c$ everywhere in the current carrying region. The analysis presented in this paper indicates that solutions of Bhagwat and Chaddah for transverse cylindrical samples correspond to choosing $n = 2$.

In the absence of an exact expression for surface current density on conductors of finite size and arbitrary shape, the method presented here remains valid only for transverse cylindrical samples. The problem of determining current density on finite conductors would also be interesting from the point of view of magneto-statics and it would be worth expending theoretical efforts in this direction. However, recently, an integral equation approach,

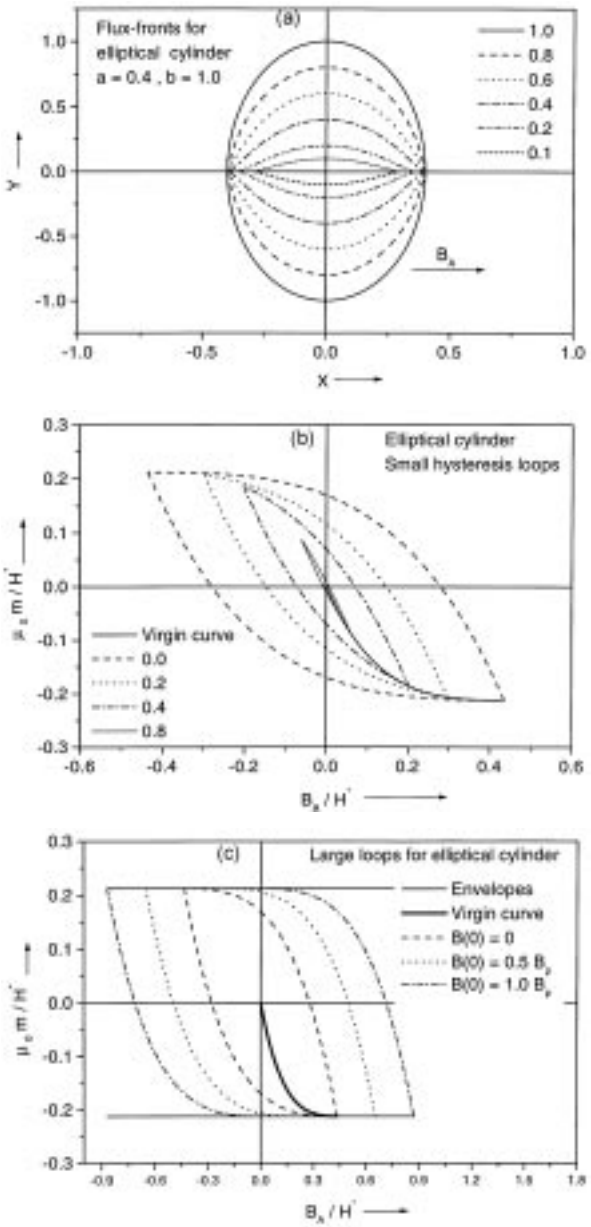

Figure 3. (**a**) The elliptical cross-section of the cylinder with semi-axes $a = 0.4$ and $b = 1$ and the flux-fronts for different values of ξ_0 are shown. (**b**) The virgin curve and typical small hysteresis loops for different reversal fields characterized by ξ_0' are shown. (**c**) The virgin curve and typical large hysteresis loops corresponding to the $B(0)/B_p = 0, 0.5$, and 1 are shown. $B(0)$ is the field at the centre of the start of reversal and $B_p = 0.435H^*$ is the field for full penetration. The envelope curves are also shown.

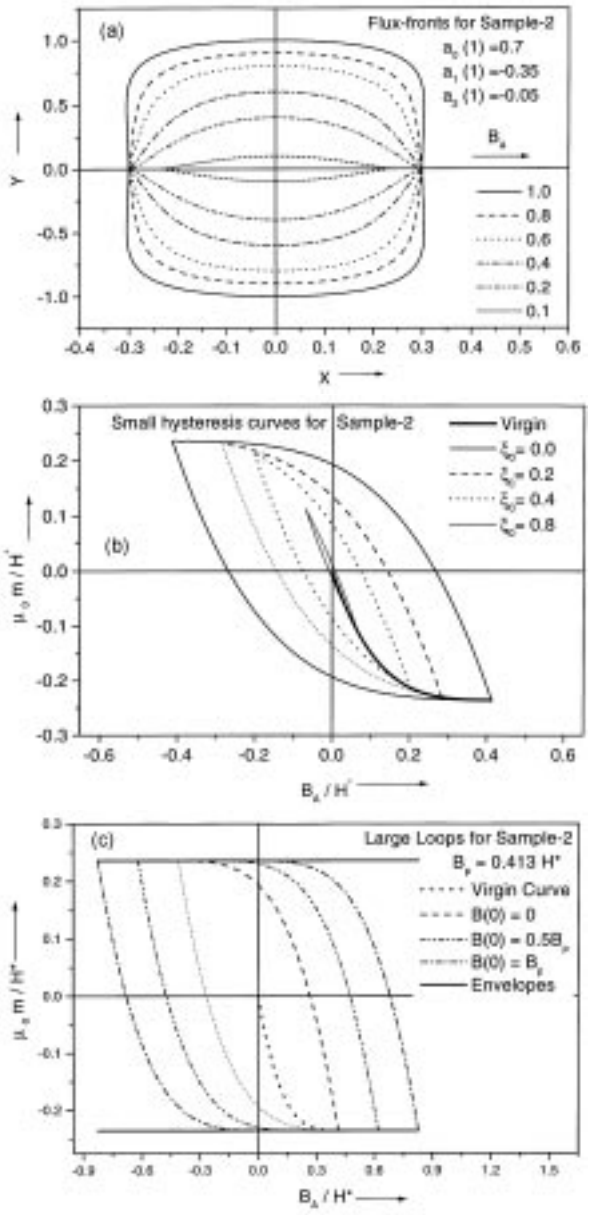

Figure 4. (**a**) The cross-section of the second cylinder and the flux-fronts different values of ξ_0 are shown. Transverse dimension $b = 1$ and the parallel dimension $a = 0.3$. The cross-sectional area $A = 1.131$. (**b**) The virgin curve and typical small hysteresis loops for different reversal fields characterized by values of ξ_0' are shown. (**c**) The virgin curve and typical large hysteresis loops for the $B(0)/B_p = 0,\ 0.5$, and 1 are shown. $B(0)$ is the field at the centre at the start of field reversal and $B_p = 0.413H^*$ is the field for full penetration. The envelope curves are also shown.

with the kernel expressed in terms of the elliptic functions, has been derived and illustrated for magnetization of a spherical sample by Telchow and Koo [16], and should prove useful for finite samples.

References

[1] C P Bean, *Rev. Mod. Phys.* **36**, 31 (1964)
[2] G Ravikumar, K V Bhagwat, V C Sahni, A K Grover, S Ramakrishnan and S Bhattacharya, *Phys. Rev.* **B61** R6479 (2000)
[3] Y Kato, M Hanakawa and K Yamafuji, *Jpn. J. Appl. Phys.* **15**, 695 ((1976)
[4] M N Wilson, *Superconducting magnets* (Oxford, Clarendon Press, 1963)
[5] K V Bhagwat and P Chaddah, *Pramana – J. Phys.* **33**, 521 (1989); also *Physica* **C224**, 155 (1994)
[6] P N Mikheenkov and Yu E Kuzovlev, *Physica* **C204**, 229 (1993)
[7] E H Brandt and M Indenbom, *Phys. Rev.* **B48**, 12893 (1993)
[8] J Mc Donald and J R Clem, *Phys. Rev.* **B53**, 8643 (1996) and references therein
[9] K V Bhagwat and P Chaddah, *Physica* **C280** 52 (1997)
[10] D V Shantsev, Y M Galperin and T H Hohansen, *Phys. Rev.* **B60**, 13112 (1999)
[11] K V Bhagwat and P Chaddah, *Physica* **C190** 444 (1992)
[12] R Navarro and L J Campbell, *Phys. Rev.* **B44** 10146 (1991)
[13] L Prigozhin, *J. Comp. Phys.* **129**, 190 (1996)
[14] E H Brandt, *Phys. Rev.* **B54** 4246; **58** 6506 (1998)
[15] M Ashkin, *J. Appl. Phys.* **50**, 7060 (1979)
[16] K L Telchow and Koo, *Phys. Rev.* **50**, 6923 (1994-II)
[17] Debjani Karmakar and K V Bhagwat, *Pramana – J. Phys.* **56**, 127 (2001)
[18] K V Bhagwat and Debjani Karmakar, *Europhys. Lett.* **49**, 715 (2000)
[19] G Polya and G Szegö, *Problems and theorems in analysis I* (Springer-Verlag, New York, 1978) p. 129–130; *Problems and theorems in analysis II* (Springer-Verlag, New York, 1971) p. 17–24
[20] H Brechna, *Superconducting magnet systems* (Springer-Verlag, Heidelberg, Berlin, 1973)
[21] Yu E Kuzovlev, *JETP Lett.* **61**, 1000 (1995)